

Darren L. Jackson*

Cooperative Institute for Research in Environmental Sciences, Boulder, CO

Brian J. Soden

NOAA Geophysical Fluid Dynamics Laboratory, Princeton, NJ

1. INTRODUCTION

Currently there is a key area of disagreement between Global Climate Models (GCMs) and satellite observations regarding the decadal-scale trends in the Earth's radiation budget. Observations from the Earth Radiation Budget Experiment (ERBE) over the period 1984-2001 indicate a trend of increasing longwave emission and increasing solar absorption at the top-of-atmosphere, which no current GCM can reproduce (Wielicki et al., 2002). Existing operational radiation budget products from TOVS conflict with the ERBE observations, in that they reveal no such trend. However, the quality and climate-scale stability of the operational TOVS satellite record is suspect largely because the processing of operational products was never performed at a level intended for detecting the decadal-scale trends of interest to the climate community. For example, the radiances were never intercalibrated between successive satellites, nor were the effects of drift in the orbital crossing times removed. Therefore, it is presently unclear if the ERBE-observed trend is real or not, and if it is real, we do not know whether it is associated with a trend in clouds or water vapor or both.

This lack of knowledge is not due to a lack of data. The HIRS radiance record provides the necessary time/space coverage, spectral resolution, and cross-instrument redundancy to resolve this discrepancy, but to date have not been processed in a manner suitable for long-term climate studies. We begin to address this issue by first reprocessing the HIRS using a consistent cloud clearance algorithm. By processing the ascending and descending orbits separately, we illustrate the impacts of drifts in the equatorial crossing time the satellites on the long-term stability of the satellite record and outline preliminary results from a method designed to correct for this spurious drift.

Correcting for orbital drifts on the NOAA polar-orbiting satellites has been done for the MSU instrument. Christy et al. (1998) use a regression method that compares differences in drift between afternoon and morning NOAA satellites. Mears et al. (2002) goes a step further and uses a general circulation model to predict MSU observations so that drifting MSU observations can be adjusted to a fixed

point in the diurnal cycle. This study incorporates elements of both methods to apply diurnal correction to the HIRS observations.

Table 1: Satellite names, time range and Local Solar Time (LST) of the ascending nodes for the HIRS data used in this study. The afternoon satellites (2 am/pm) are designated with *a*, and morning satellites (8 am/pm) are designated with *m*.

NOAA Satellite	Time period	Initial Ascending Crossing Time
TIROS-N	11/1978 - 1/1981	1500 LST _a
NOAA-6	7/1979 – 3/1983	1930 LST _m
NOAA-7	7/1981 – 1/1985	1430 LST _a
NOAA-9	1/1985 – 9/1988	1420 LST _a
NOAA-10	12/1986 – 8/1991	1930 LST _m
NOAA-11	11/1988 - 12/1994	1330 LST _a
NOAA-12	6/1991 – 3/1997	1930 LST _m
NOAA-14	1/1995 – 12/2001	1330 LST _a

2. DATA DESCRIPTION

Observational data from HIRS and geostationary satellites and GFDL model data were utilized for this study. The following section provides background information for these data.

2.1 HIRS data

The High-resolution Infrared Radiation Sounder (HIRS) has flown aboard NOAA polar-orbiting satellites since 1978. HIRS is a cross-track scanner with 19 narrow-band IR channels and one visible channel and has the primary purpose of retrieving temperature and water vapor profiles. The HIRS 1b data were converted from raw counts to brightness temperature using the International TOVS Processing Package (ITPP) version 5.20. The data period used in this study began November 1978 and ended December 2001 with the radiances originating from HIRS/2 sensors riding onboard eight separate NOAA polar-orbiting satellites. Table 1 lists information on the satellites used in this study. No data were used

* Corresponding author address: Darren L. Jackson, NOAA/ETL, 325 Broadway R/ET6, Boulder, CO 80305-3328; e-mail: Darren.L.Jackson@noaa.gov

from NOAA-8 because of its less than 2 year lifespan, and no data were used from HIRS/3 sensors found onboard the most recent NOAA satellites starting with NOAA-15.

2.2 Geostationary Data

Geostationary data combined from multiple satellites over a one-year period (1999) were included in the analysis to validate the HIRS-sampling bias caused by the drift the NOAA polar-orbiting satellites. A 3-hour time step with the geostationary data allowed for complete diurnal sampling, while combining multiple satellites (GOES-8, GOES-10, GMS-5, METEOSAT-5, and METEOSAT-6) provided for the global coverage.

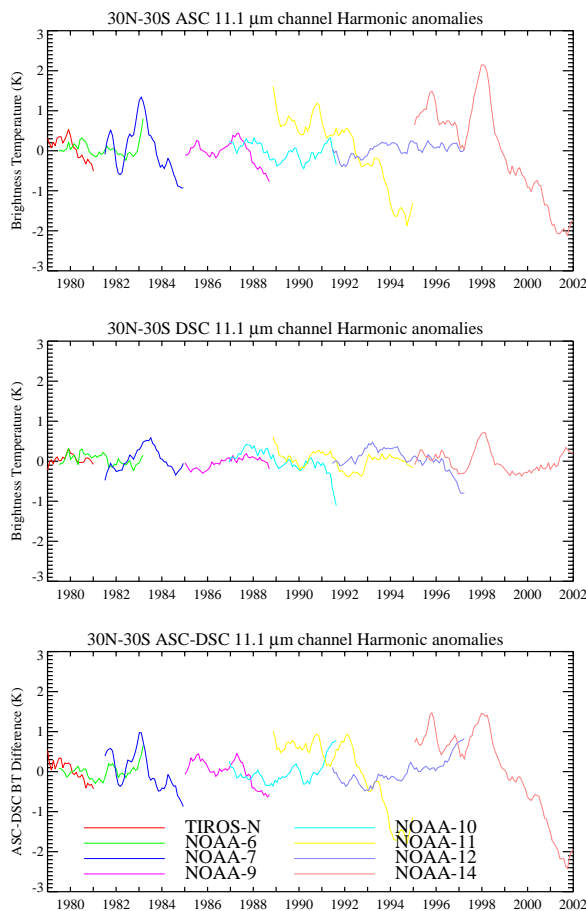


Figure 1: Time series of HIRS ascending (ASC), descending (DSC), and ascending-descending anomalies for the 11.1 μm channel.

2.3 HIRS Simulated Data

HIRS simulated model data originated from the GFDL Atmospheric Model 2 (AM2). Further details regarding the model configuration and comparison of its simulated climate with observations are provided in Anderson et al. (2004). AM2 uses a new grid point

dynamical core with a staggered Arakawa B-grid of 2.5° longitude by 2° latitude spacing. The hybrid vertical coordinate combines sigma surfaces near the ground and smoothly transitions to pressure surfaces above 250 hPa. The number of vertical layers ranges between 18 and 24 depending upon the version of AM2 used. Shortwave radiation accounts for gaseous absorption by H_2O , CO_2 , O_3 , and O_2 , molecular scattering, and absorption and scattering by aerosols and clouds. Longwave radiation accounts for absorption and emission by H_2O , CO_2 , O_3 , N_2O , CH_4 , and halocarbons. Moist convection is parameterized using a version of Relaxed Arakawa-Schubert while large-scale clouds are represented with prognostic variables for cloud fraction and the liquid and ice specific humidities, with microphysics parameterized according to Rotstajn (1997).

The model is integrated using observed sea-surface temperatures and time-varying trace gas and aerosol species for the period 1978-2002. Instantaneous fields of temperature, water vapor, and clouds are stored every 3 hours and then inserted (offline) into a narrow-band radiative transfer model to simulate the radiance which would be observed by the satellite under those atmospheric conditions. The model used here is the HIRS Fast Forward Program (HFFP) which has been shown to agree with line-by-line calculations to within 0.1 K (Soden et al., 2000). These simulations provide global, 3-hourly radiances for both clear and total-sky conditions for all spectral channels on each individual HIRS instrument flown for the period 1978-2002 (see Table 1).

3. DIURNAL CORRECTIONS

This section gives evidence of the diurnal sampling problem in the HIRS data and provides a method for correcting this problem.

3.1 Data Grids

The HIRS all-sky brightness temperature swath data were averaged onto monthly 2.5° grids. HIRS monthly averages were applied only to the near-nadir observations (scan positions 26-31) so to remove any bias introduced by limb effects. The HIRS data grids were further separated into ascending-only and descending-only monthly grids. Separating ascending and descending passes eliminated averaging observations at different diurnal times. All HIRS monthly grids contained information on the standard deviation, the number of observations, and the time of each observation for each grid cell. The latter information was essential in creating a HIRS-sampled data set from the model and geostationary data. Monthly brightness temperature data grids were further categorized by satellite and channel. While HIRS observations from the tropospheric temperature channels near $15 \mu\text{m}$ and the water vapor channels near $6.7 \mu\text{m}$ were processed for this study, only results from $11.1 \mu\text{m}$ surface temperature channel are presented in this paper.

Monthly-mean ascending and descending grid data were further processed into monthly interannual anomaly fields. Analyzing Interannual anomalies helped isolate the signal of diurnal drift. A time series of HIRS ascending and descending brightness temperatures for given satellite, channel, longitude, and latitude can be defined as

$$T_b^{ASC} = \overline{T_b^{ASC}} + \hat{T}_b^{ASC} \quad (1)$$

$$T_b^{DSC} = \overline{T_b^{DSC}} + \hat{T}_b^{DSC} \quad (2)$$

Where left side of each equation represents the total field for each orbital node and the right side of each equation gives the mean (total mean + annual cycle) and interannual anomaly fields. The first three harmonics are computed to represent the annual cycle. This method required filling any time series with missing data by interpolation. Interpolation was conducted only for grid boxes containing valid data for more than 75% of the time series. Other quality controls required month mean averages at each grid cell to contain at least 30 observations/month and for each time series to have standard deviation less than 25K.

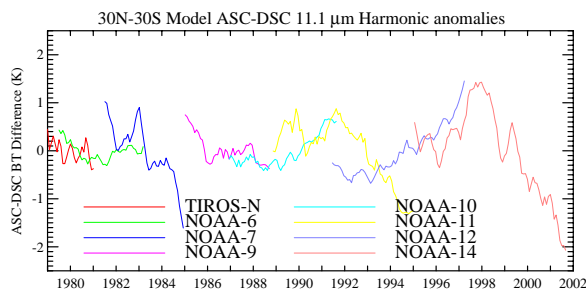
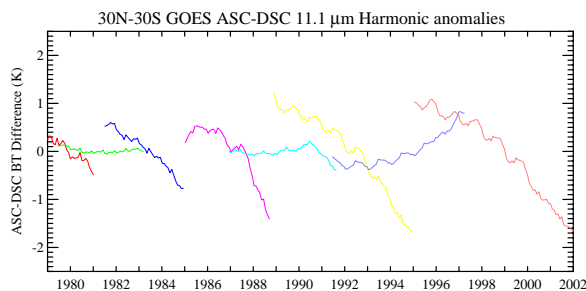
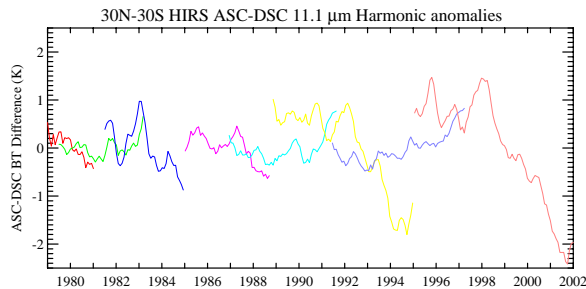


Figure 2: Time series of ascending-descending anomalies from HIRS, geostationary, and GFDL model.

GFDL model and geostationary data were sub-sampled using the observations time from the HIRS ascending and descending grid data. Along with these sub-sampled grids, monthly mean and anomaly grids were constructed using all of the 3-hourly model and geostationary data. These data represent monthly averages and anomalies that are not affected by changes in HIRS sampling caused by orbit drift.

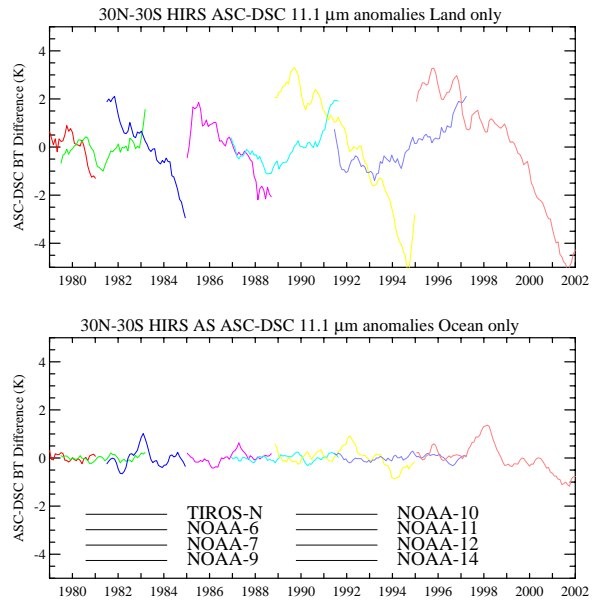


Figure 3: Time series of ascending-descending anomalies from HIRS for land-only and ocean-only observations.

3.2 Observed Diurnal Sampling Drift

To examine if we can detect a HIRS diurnal sampling bias, we first examined time series of the HIRS ascending and descending averages for the 11.1 μm channel. Figure 1 gives the ascending, descending and ascending-descending for the HIRS all-sky observations at this channel for the 30N-30S domain. The ascending anomalies show the greatest diurnal drift from the afternoon (2pm) NOAA satellites. As the local crossing time of the afternoon satellites drifts forward in local time, the surface sensing channels respond by cooling. The descending (8am) morning satellites observations also show cooling near the end of the period for NOAA-10 and -12. The morning satellites drift backward in local time, so this cooling agrees the expected changes in diurnal temperature near morning. The much smaller temperature change of the morning satellites is expected since these satellites drift at slower rate than the afternoon satellites. Descending afternoon orbits (2am) show little diurnal drift since most the drift

occurs at night where diurnal temperatures changes are small. Taking the difference between the ascending and descending nodes illustrates that both morning and afternoon satellites experience diurnal drift with largest drifts occurring for the NOAA-11 and NOAA-14 afternoon satellites.

To determine if this effect is truly caused by changes in HIRS sampling, a comparison was made with the HIRS-sampled geostationary and model data for the ascending-descending difference. Figure 2 shows the magnitude and direction of the diurnal drift is well captured by both geostationary satellite observations and model simulations. Agreement between HIRS and model data is greatest for NOAA-10,-11,-12, and -14, but some deviation does occur at the end of the NOAA-7 and beginning of the NOAA-9 period. GOES 11.1 μm data further validates the magnitude and direction of the HIRS diurnal sampling drift and the model simulated drift. Since only one year of geostationary data were sub-sampled over the multiple years of HIRS data, the lack of interannual variations in the geostationary data creates smoother curves.

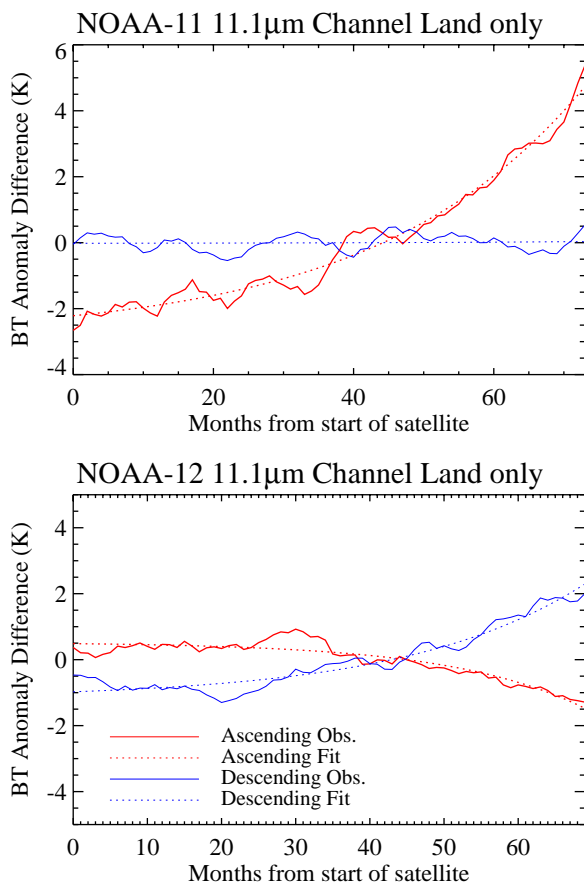


Figure 4: Time series indicating functional fit to anomaly difference (total anomaly – ascending/descending anomaly).

The diurnal sampling drift was further dissected into land-only and ocean-only components. Figure 3 shows the HIRS 11.1 μm land-only observations contribute almost the entire signal in diurnal drift seen in Figure 2. The ocean-only case does not readily show changes in diurnal sampling, but does show an interannual ENSO signal in the temperature field with maxima occurring in the difference field during El Niño events. Therefore, Figures 2 and 3 indicate that any correction applied to HIRS channels with surface sensitivity need to account for surface effects.

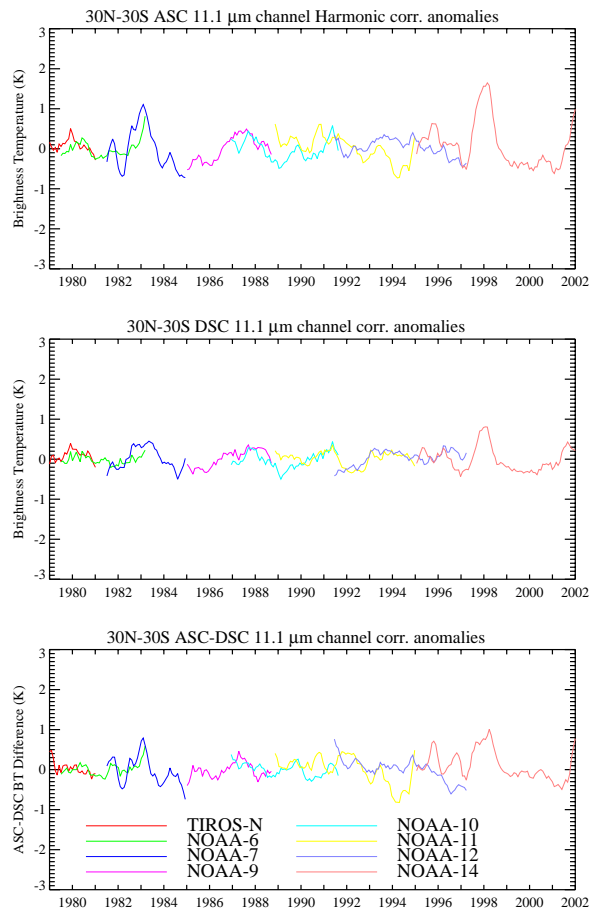


Figure 5: Same as Figure 1 except the HIRS anomalies have been corrected for diurnal sampling bias.

3.3 Diurnal Correction Method

Since model simulations capture the drift of the HIRS diurnal drift, a diurnal correction was defined by subtracting the ascending and descending anomalies from the total model anomaly field. The correction described in this paper is defined to correct the zonally-averaged data shown in Figures 1 and 2. Therefore, this difference was defined as function of satellite, orbit node, surface type, channel, latitude band, and time from the model simulations and then

applied to the HIRS observations to correct for the diurnal drift. In principle, this correction could be applied as a function of both latitude and longitude which is the ultimate goal of this study. The advantage of the diurnal correction being applied at the grid cell level would be that the correction could be applied to the HIRS swath data rather than zonal averages.

Diurnal corrections were constructed using model time series differences between the total anomaly and each of the HIRS sub-sampled ascending or descending anomaly grids. Figure 4 gives an example of this difference for data averaged over the 30N-30S domain. The fitting routine used a three-parameter exponential fit of the form

$$\Delta T_b^{ASC} = T_b^{\wedge Total} - T_b^{\wedge ASC} = a_0 + a_1 e^{a_2 \cdot t} \quad (3)$$

$$\Delta T_b^{DSC} = T_b^{\wedge Total} - T_b^{\wedge DSC} = b_0 + b_1 e^{b_2 \cdot t} \quad (4)$$

Where ΔT_b^{ASC} and ΔT_b^{DSC} are the differences between the total anomaly and each orbital node, coefficients a_0 , a_1 , a_2 , b_0 , b_1 , b_2 , and b_3 represent the fitting parameters, and t represents time in months. ΔT_b^{ASC} , ΔT_b^{DSC} , and coefficients are a function of satellite, channel, surface type, latitude band, and time. This functional form best matched the shape of the diurnal drift for the NOAA polar-orbiting satellites seen in Figure 4. Coefficients were determined using a gradient expansion algorithm. When chi-square did not converge in the algorithm, it resulted in no correction being applied to the data. These cases occurred primarily for the HIRS upper tropospheric temperature channels, oceanic regions, and descending nodes where diurnal influences were small. Coefficients a_0 and b_0 represent the anomaly difference between the total anomaly and ascending/descending anomaly shortly after launch of the satellite. Including the a_0 and b_0 parameters in the correction depends on whether you want the HIRS corrected radiances to be based on the local solar time shortly after launch or on the diurnal averaged anomalies over the 24-hour period.

The correction can be applied to each ascending and descending anomaly grids to create a new corrected HIRS brightness temperature anomaly field using

$$T_b^{\wedge ASC, adj} = T_b^{\wedge ASC} + \Delta T_b^{ASC} \quad (5)$$

$$T_b^{\wedge DSC, adj} = T_b^{\wedge DSC} + \Delta T_b^{DSC} \quad (6)$$

And this field can be used to adjust the mean field by simply adding the result of (5) into (1) and (6) into (2). Figure 5 shows the adjusted time series for the HIRS 11.1 μm channel. Ascending orbits for the afternoon

satellites no longer show the diurnal drift seen in the Figure 1. Small drifts near the end of the descending orbits for NOAA-10 and NOAA-12 also show the correction removing diurnal bias. Interannual variations have been preserved as can be seen by the warming in 1983 and 1997 associated with El Niño.

4. CONCLUSIONS

The effects of orbit drift in the HIRS all-sky data are identified utilizing GFDL model simulations. Sampling bias in the HIRS data was reproduced in the GFDL model simulation and found particularly large for surface-sensitive channels for the afternoon satellites. Removal of diurnal drift from the HIRS radiance data could improve our assessment of climate parameters derived from HIRS such as temperature, water vapor, clouds, and OLR.

Future plans include creating HIRS bias corrections that are function of both longitude and latitude so that corrections can be applied to the HIRS swath data. All-sky corrections will be compared to clear-sky corrections to see what effects the clouds have on the diurnal bias. Following correction of both diurnal and inter-satellite biases, HIRS observations and retrieval products should give a more accurate assessment of global climate change.

5. REFERENCES

- Anderson et al. (2004)
- Christy, J.R., R.W. Spencer, and E.S. Lobl, 1998: Analysis of the merging procedure for the MSU daily temperature time series. *J. Climate*, **11**, 2016-2041.
- Mears C.A., M.C. Schabel, and F.J. Wentz, 2002: *Proceedings of the International Geophysics and Remote Sensing Symposium*, Volume III, pg. 1839-1841
- Rotstain, L. D., 1997: A physically based scheme for the treatment of stratiform clouds and precipitation in large-scale models. I: Description and evaluation of the microphysical processes. *Quarterly Journal of the Royal Meteorological Society*, **123A** (541): 1227-1282.
- Soden, B. and Co-authors, 2000: An intercomparison of radiation codes for retrieving upper tropospheric humidity in the 6.3-micron band: A report from the 1st GVaP workshop. *Bull. Amer. Meteor. Soc.*, **81**, 797-808
- Wielicki and Co-authors, 2002: Evidence for large decadal variability in the tropical mean radiative energy budget. *Science*, **295**, 841-844